Enhancement of spin relaxation time in hydrogenated graphene spin-valve devices

Wojtaszek, M.; Vera-Marun, I. J.; Maassen, T.; van Wees, B. J.

Published in:
Physical Review. B: Condensed Matter and Materials Physics

DOI:
10.1103/PhysRevB.87.081402

Publication date:
2013

Supplemental Material

Enhancement of spin relaxation time in hydrogenated graphene spin valve devices.

M. Wojtaszek,[1] I. J. Vera-Marun,[1] T. Maassen,[1] and B. J. van Wees[1]

[1]*Physics of Nanodevices, Zernike Institute for Advanced Materials, University of Groningen, Groningen, The Netherlands**

PACS numbers: 72.25.-b, 85.75.-d

I. SPIN VALVE MEASUREMENTS UPON HYDROGENATION. CHANGES OF CONTACT POLARIZATION.

To properly resolve the switching of individual Co contacts when sweeping the magnetic field we vary the width of fabricated contacts from 125 nm to 250 nm. The non-local spin valve measurements are always performed using the outermost contacts as a current drain and voltage detector reference. R_{NL} in the fabricated devices shows small (<10%, in case of device B with all ferromagnetic contacts) or non (device A, with non-magnetic outer contacts) extra switches. The presence of only two different resistivity levels in non-local spin valve measurements confirms that the outer detector as well as the current drain do not affect the spin resistivity (no additional switches are observed in spin valve signals).

We observe that upon hydrogenation the contact resistances always increase (by 10-50%) and the polarization of contacts variously changes. Figure 1 shows that the contact polarization can decrease (lower panel) or even switch the polarization (upper panel). Such inversion of contact polarization can be explained by the change of the tunneling interface of the contact during the hydrogenation process, by for example the depletion of oxygen within AlO_x tunneling barrier. Similar effect we also observe in the thermally treated ferromagnetic contacts, which will be described in our future publication (I.J.Vera-Marun *et al.* in preparation).

In any of the room temperature non-local spin valve measurement (Fig. 1) we do not observe a decrease of R_{NL} around zero magnetic field, which one would expect for uncorrelated magnetic dipole moments originating from hydrogen defects[1,2]. From this we conclude that at the defect concentration estimated here ($4.5\text{x}10^{11}$ atoms/cm^2) magnetic moments associated with hydrogen defects do not introduce any significant magnetic field or that this effect is randomized by the thermal fluctuations (we note that the spin valve displaying such an effect were measured at low temperatures[1,2], below 15 K).

II. FABRICATION AND CURRENT SPECTROSCOPY OF TUNNELING CONTACTS

The cobalt electrodes are patterned using electron beam lithography and after the development of the resist the layers of Al and Co are evaporated. Before the evaporation

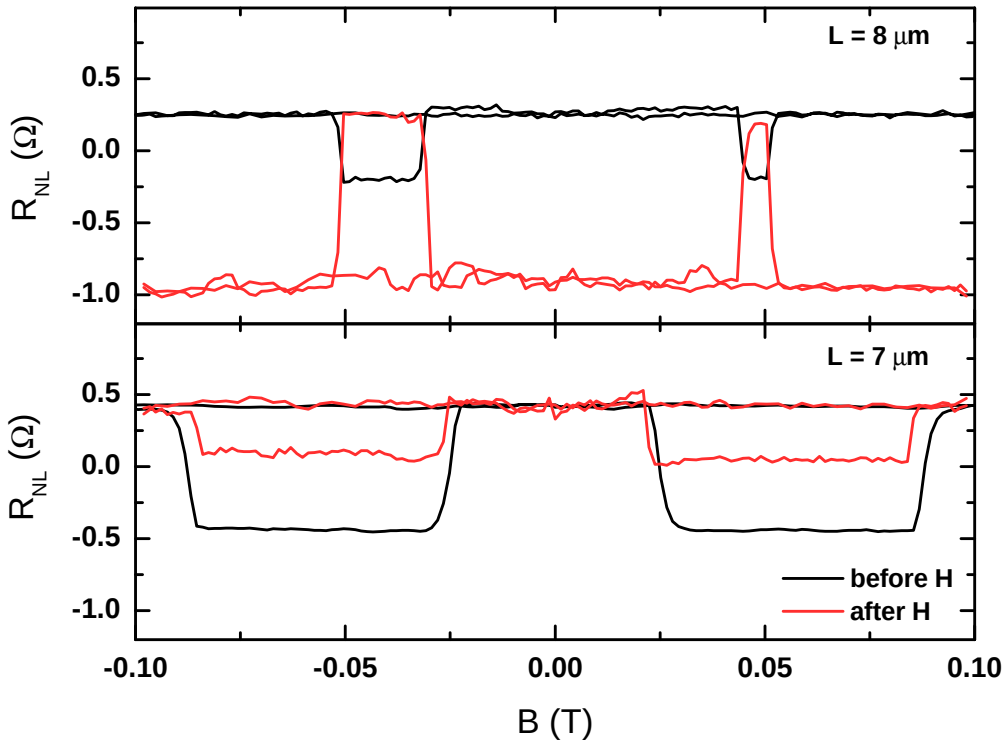

FIG. 1: (Color online) Spin valve measurement in graphene over two different distances before and after hydrogenation (trace and retrace, with the saturation field of 0.5 T) in device B. The hydrogenation process affects contact polarization, decreasing it (bottom panel), increasing it or even changing the sign of polarization (top panel). This can be explained by a change of the interface of the contact, like the depletion of oxygen within the Al_2O_3 tunneling barrier during the plasma hydrogenation of the device.

of a thin layer of Al for tunneling barrier, when the sample is still screened from the e-beam target by the shutter, we pre-evaporate 10 nm of Ti to lower the base pressure in the chamber (1x10^{-6} mbar). This procedure might deposit a fractional monolayer of Ti on the sample, which would act as a seeding layer for Al and improves the smoothness of the tunneling interface[3]. AFM measurements of the Al film on graphene with and without Ti pre-evaporation, however, show no significant difference in roughness: in both cases the root mean square of surface roughness ranges between 0.4 and 0.6 nm. Therefore we rule out any effect of the Ti pre-evaporation other than the intended reduction in base pressure.

The 3 terminal resistances of the contacts R_C in device A fall in the range from ∼10 to ∼50 kΩ. The optimal range value of contact resistances plays an important role in reducing

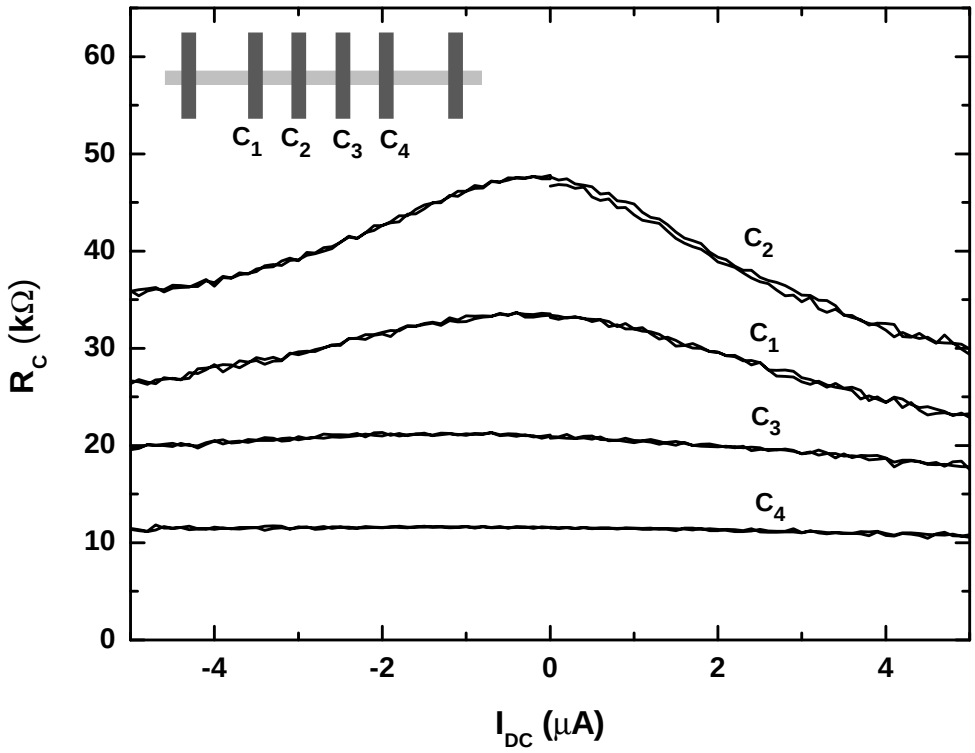

FIG. 2: (Color online) Current spectroscopy of tunneling contacts in a graphene spin-valve device (device A) and their schematic position in the device. All the contact resistances are above 10 kΩ and their individual values scale with the designed contact area, indicating homogeneous contact resistivity. The contacts display a non-linear change in resistivity with the current bias, most pronounced for the highest resistive contacts. This indicates a tunneling injection through the interface.

the conductivity mismatch between a metal electrode and graphene and suppressing the backscattering of spins into the contacts, so that a detectable spin accumulation can be achieved. To quantify that we calculate R parameter $R = R_C W/\rho$, introduced in Ref. 4, where ρ is the graphene resistivity and $W = 1.5$ μm is the flake width. This parameter represents the strength of the spin relaxation due to the finite contact resistances and indicates the deviations from exponential decay of the spin signal with the distance for R <1x10^{-6}m. For the contacts in our devices the R parameter ranges from 3x10^{-6}m to 1x10^{-4}m and explains why we observe non-local signals as high as R_{NL}=20 Ω at a distance of 1.3 μm.

To confirm the tunneling character of the contacts, we measure the change of differential contact resistance under DC bias. For that we apply in a 3 terminal configuration, where the

source and voltage probe are using the same electrode, a variable DC current I_{DC} with an AC component of 100 nA (to be detected by a Lock-In amplifier). As can be seen in Fig. 2, the non-linear behavior is most significant for the highest resistive contact (C_2), though even for the least resistive one (C_4) the measurement displays small non-linearity with I_{DC}. This indicates the tunneling injection through the ferromagnetic contact and explains high spin signals and spin transport properties (τ_S, D_S) in the measured devices.

III. COMPARISON BETWEEN D_S AND D_C WITH BROADENED DENSITY OF STATES.

The diffusion coefficient can be independently extracted from charge (D_C) and from spin (D_S) transport. D_C is calculated using the Einstein relation $\sigma = e\ \nu(E) D_C$, where $\nu(E)$ is the density of states and $\sigma = 1/\rho$ is the graphene sheet conductivity. In the theoretical limit of T = 0 K the number of states at the Dirac point in ideal graphnene vanishes and that leads to a singularity of D_C at V_D. This can be eliminated by introducing a Gaussian broadening to $\nu(E)$, which collectively accounts for finite temperature, electron-hole puddles and possibly finite lifetime of electronic states[5]. In our case, the good agreement between D_C and D_S before hydrogenation is obtained when $\tilde{\sigma} = 110$ meV, see Fig. 3, and is close to the values reported in the literature[2,5]. Though with the same value of $\tilde{\sigma}$ one can qualitatively imitate the behavior of D_S also after hydrogenation, we observe a slight offset between D_C and D_S of 0.002 m^2/s,, which cannot be compensated by a further increase of $\tilde{\sigma}$. In the sparse low temperature data (T = 70 K for device A, T = 4K for device B) we also do not observe any significant discrepancy between the values of D_C and D_S.

Such a discrepancy can originate from the presence of localized states in graphene or its close vicinity[6] or by the modulation of the gyromagnetic ratio due to the effective magnetic field from magnetic moments induced by hydrogen defects[2]. The latter case does not apply here because at room temperature the thermal fluctuations randomize these localized magnetic moments. As we do not observe a dip in spin-valve measurements of R_{NL} at low magnetic field neither the difference between D_C and D_S we do not expect a change in the g-factor. Following the discussion in Ref. 2 the eventual enhancement of the g-factor at room temperature is estimated to be less than 2 %, therefore it is reasonable to use the free-electron value $g = 2$ in Hanle fits. From that we conclude that the probable reason for a

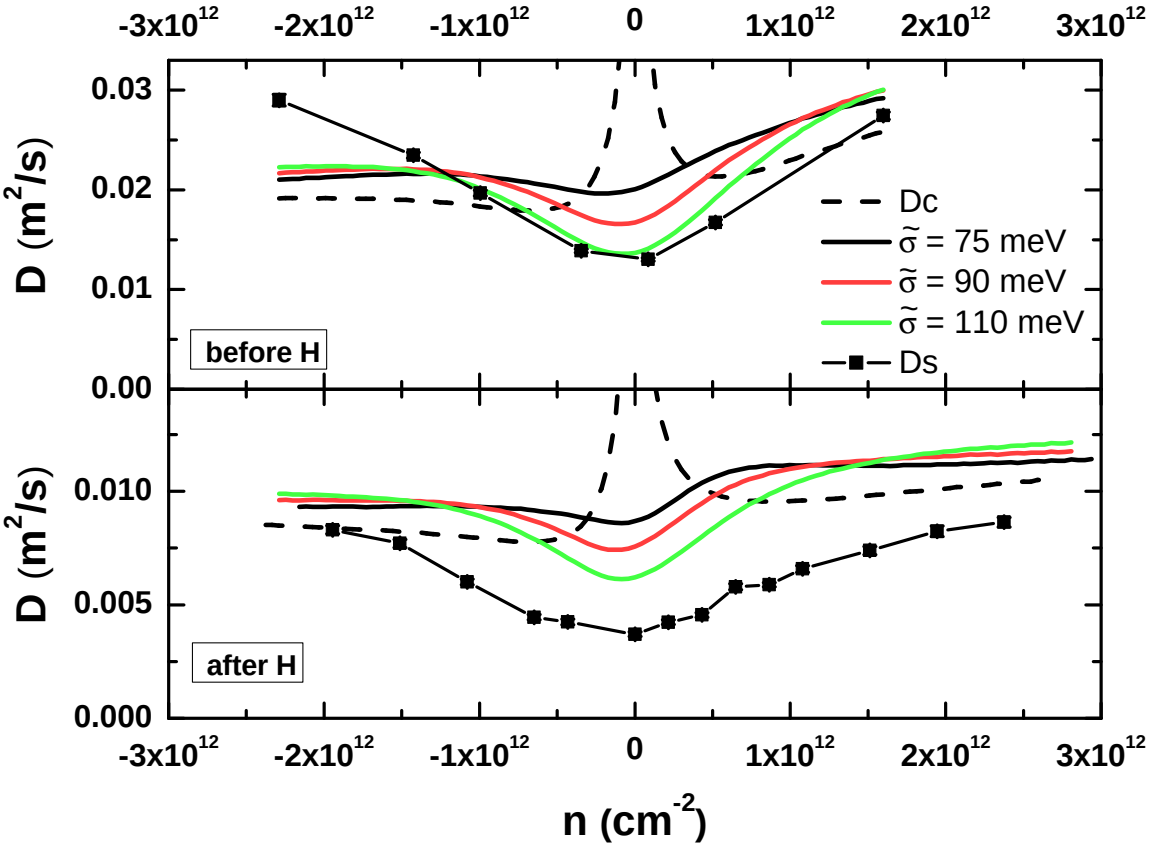

FIG. 3: (Color online) Comparison of the diffusion coefficient extracted from charge-D_C and from spin-D_S transport measurements, before and after hydrogenation for device A. Dashed lines display D_C calculated for density of states $\nu(E)$ without any broadening, continues lines display D_C obtained when a Gaussian broadening of $\tilde{\sigma}$ is introduced to the $\nu(E)$. The square points represent the diffusion coefficient obtained from Hanle precession measurements (D_S). A good agreement between D_C and D_S is obtained for $\tilde{\sigma} = 110$ meV for the case before hydrogenation. After hydrogenation there is an offset between D_C and D_S of 0.002 m^2/s, which cannot be compensated by a further increase of $\tilde{\sigma}$.

small offset of D_S with respect to D_C after hydrogenation is the modulation of the density of states due to localized states. Nevertheless, the general similarity between D_S (from Hanle fits) and D_C (calculated using the standard graphene DOS) confirms that the DOS in softly hydrogenated graphene is not significantly affected.

IV. HANLE MEASUREMENTS FOR DIFFERENT DISTANCES BETWEEN INJECTOR AND DETECTOR.

We present the details of the elementary fits and extracted coefficients for different distances L between injector and detector. In device A the measured spacings are L=1.3, 3.3 and 5.5 μm; in device B L= 1.5, 3, 4, 6.5, 7, 8 and 11 μm. In Fig. 4 and Fig. 5 we present three representative regions of each device. The obtained spin coefficients are very similar within the individual set (before or after hydrogenation). In most of the data we apply the fitting procedure to the difference between the Hanle precession measurements at parallel and antiparallel magnetizations to keep the fitting offset at zero.

Additionally, to ensure the quality of the fits and the independent extraction of the spin coefficients D_S and τ_S from the fitting procedure, we perform an alternative fitting approach. We execute the fitting for fixed values of diffusion D_S=D_C, where D_C is extracted from charge transport in the metallic regime using the Einstein relation for the ideal DOS. This approach leads to the very similar values of τ_S (within 20% difference, see Fig. 6b), however obtained fits are less accurate, especially at the shoulders of Hanle curves (see Fig. 6c). This analysis ensures that the fitting approach and obtained spin coefficients are consistent and determined trustworthy.

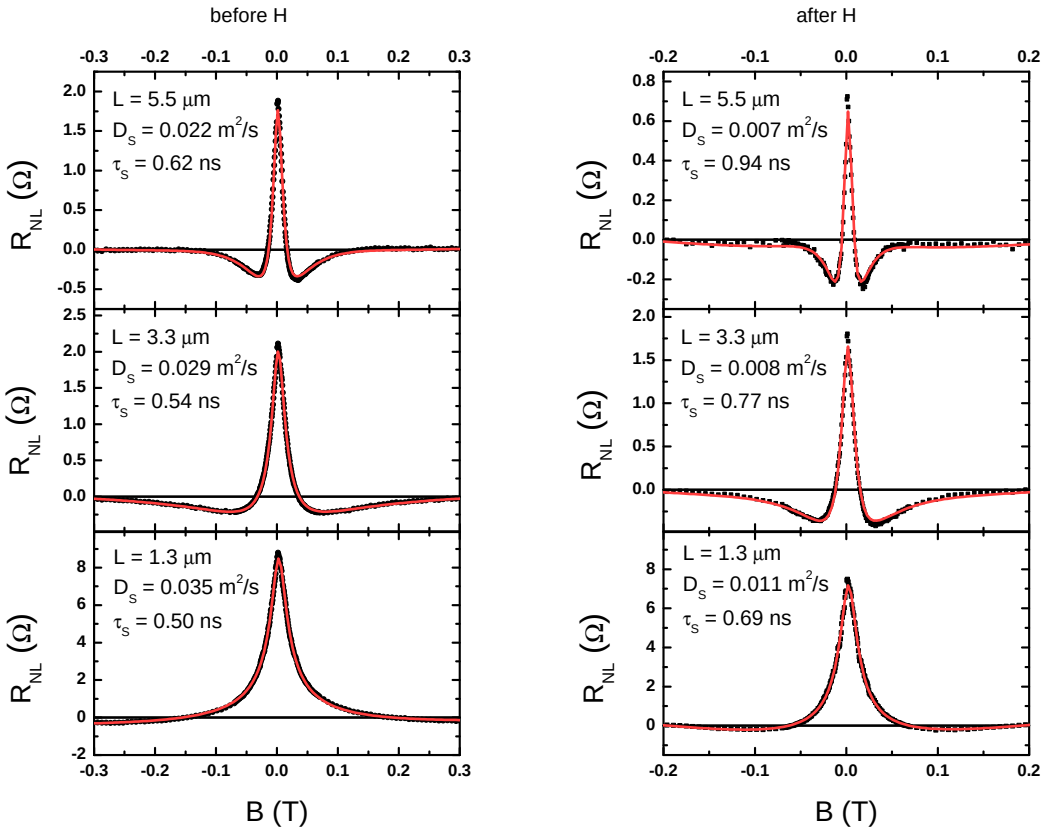

FIG. 4: (Color online) Hanle precession curves of device A for three different distances L between injector and detector, (a) before hydrogenation, (b) after hydrogenation. Red line represents the fits of the data to Bloch equation and extracted spin coefficients are displayed next to the corresponding data. All presented data are obtained for carrier concentration $n = 2.3\text{x}10^{12}$ cm^{-2} ($V_g - V_D = 53$ V). Notice the different scales of the magnetic field before and after hydrogenation.

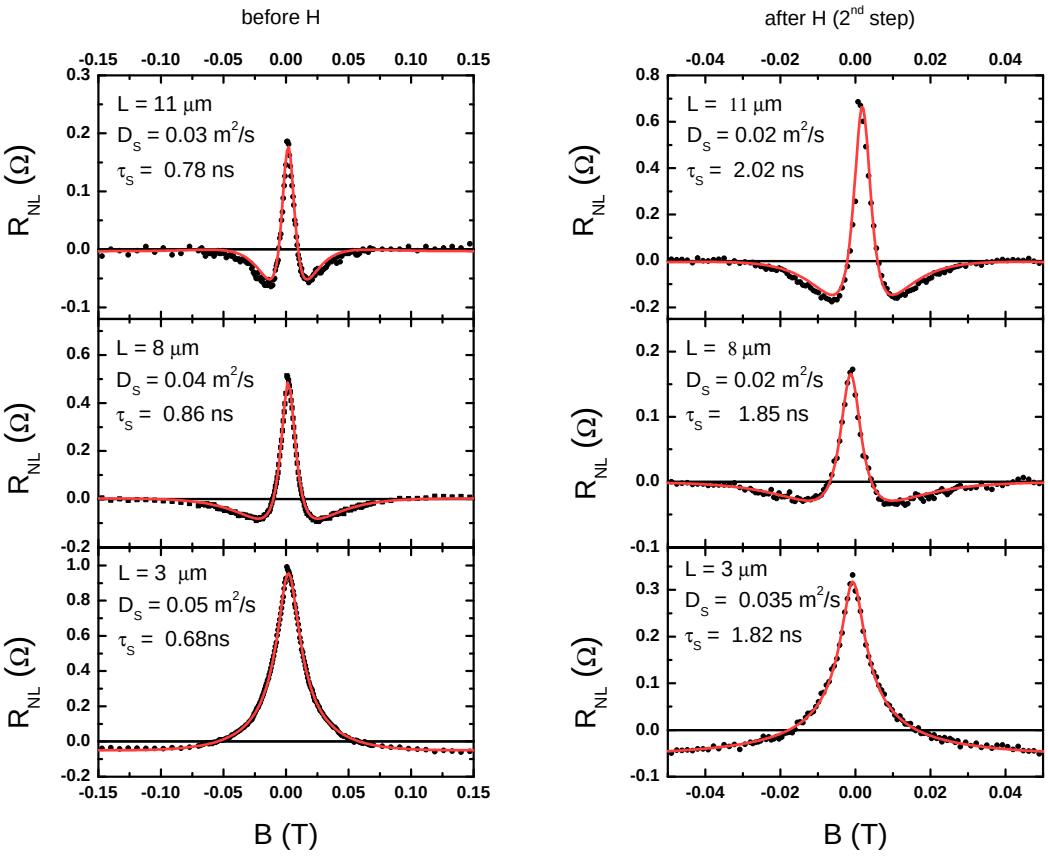

FIG. 5: (Color online) Hanle precession curves of device B for three different distances L between injector and detector, (a) before hydrogenation, (b) after 2^{nd} hydrogenation step. Red line represents the fits of the data to Bloch equation and extracted spin coefficients are displayed next to the corresponding data. All presented data are obtained for carrier concentration $n = 2.2\text{x}10^{12}$ cm^{-2}. Notice the different scales of the magnetic field before and after hydrogenation.

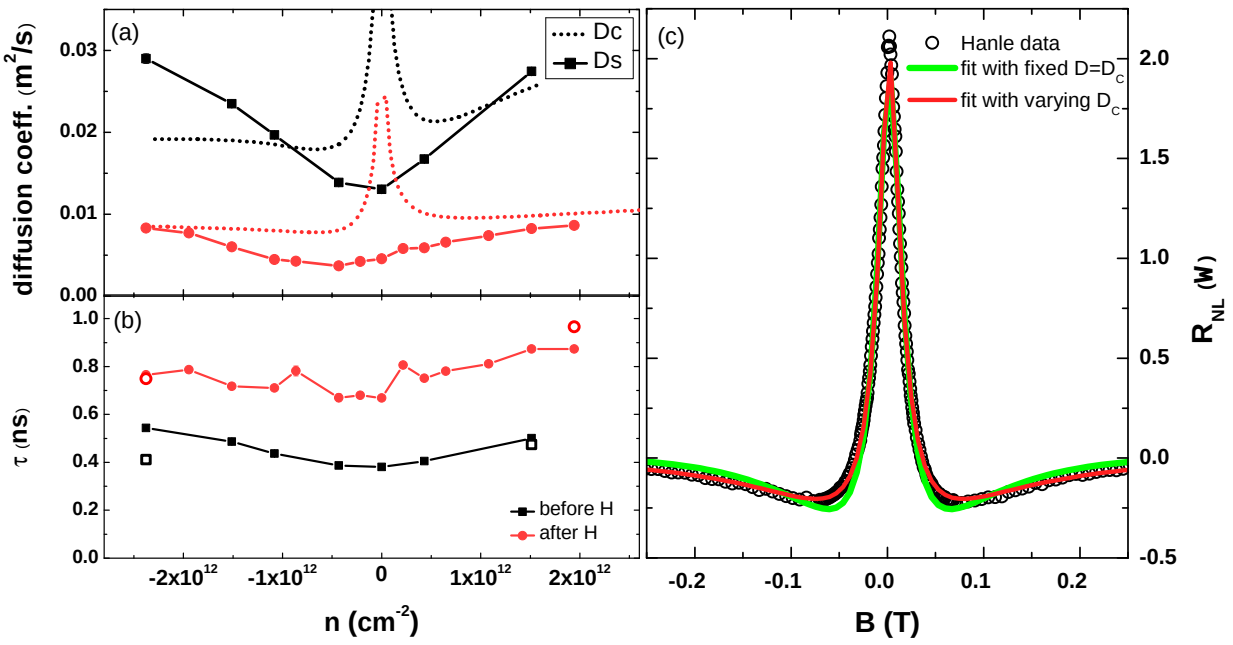

FIG. 6: (Color online) (a, b) Reproduction of Fig. 2b of the main manuscript summarizing values of spin coefficients as a function of doping. Filled circles are the data obtained from fitting Hanle measurements with D_S and τ_S as a free variables. Additional data points of τ_S (open circles) are obtained by fitting Hanle measurements with fixed values of D_S=D_C, where D_C is calculated from charge transport using the Einstein relation for the ideal DOS in the corresponding metallic regime. (c) Example of Hanle precession data (device A, before H, n = 2.3x10^{12} cm^{-2}.) together with two different fitting curves, one obtained when both D_S and τ_S were free variables, the other by keeping the diffusion constant fixed (D_S=D_C). Although discrepancies between both fitting methods are below 20%, the quality of the fits is better for the case with both D_S and τ_S as free variables, especially at the shoulders of Hanle curves.

* Electronic address: m.wojtaszek@rug.nl

[1] X. Lou, C. Adelmann, S. A. Crooker, E. S. Garlid, J. Zhang, K. S. M. Reddy, S. D. Flexner, C. J. Palmstrom, and P. A. Crowell, Nat. Phys. **3**, 197 (2007).

[2] K. M. McCreary, A. G. Swartz, W. Han, J. Fabian, and R. K. Kawakami, Phys. Rev. Lett. **109**, 186604 (2012).

[3] W. Han and R. K. Kawakami, Phys. Rev. Lett. **107**, 047207 (2011).

[4] M. Popinciuc, C. Józsa, P. J. Zomer, N. Tombros, A. Veligura, H. T. Jonkman, and B. J. van Wees, Phys. Rev. B **80**, 214427 (2009).

[5] C. Józsa, T. Maassen, M. Popinciuc, P. J. Zomer, A. Veligura, H. T. Jonkman, and B. J. van Wees, Phys. Rev. B **80**, 241403 (2009).

[6] T. Maassen, J. J. van den Berg, E. H. Huisman, H. Dijkstra, F. Fromm, T. Seyller, and B. J. van Wees, Phys. Rev. Lett. **110**, 067209 (2013).